

First pharmacophore-based identification of androgen receptor down-regulating agents: Discovery of potent anti-prostate cancer agents

Puranik Purushottamachar,^{a,†} Aakanksha Khandelwal,^{a,†} Pankaj Chopra,^a
Neha Maheshwari,^a Lalji K. Gediya,^a Tadas S. Vasaitis,^a Robert D. Bruno,^a
Omoshile O. Clement^c and Vincent C. O. Njar^{a,b,*}

^aDepartment of Pharmacology & Experimental Therapeutics, University of Maryland School of Medicine,
685 West Baltimore Street, Baltimore, MD 21201-1559, USA

^bThe University of Maryland, Marlene and Stewart Greenebaum Cancer Center, School of Medicine, Baltimore, MD 21201-1559, USA

^cBio-Rad Laboratories, Informatics Division, 3316 Spring Garden Street, Philadelphia, PA 19104, USA

Received 19 December 2006; revised 5 March 2007; accepted 8 March 2007

Available online 13 March 2007

Abstract—A qualitative 3D pharmacophore model (a common feature based model or Catalyst HipHop algorithm) was developed for well-known natural product androgen receptor down-regulating agents (ARDAs). The four common chemical features identified included: one hydrophobic group, one ring aromatic group, and two hydrogen bond acceptors. This model served as a template in virtual screening of the Maybridge and NCI databases that resulted in identification of six new ARDAs (EC₅₀ values 17.5–212 μM). Five of these molecules strongly inhibited the growth of human prostate LNCaP cells. These novel compounds may be used as leads to develop other novel anti-prostate cancer agents.

Published by Elsevier Ltd.

1. Introduction

Prostate cancer (PCA) is the most common type of cancer found in American men, and androgen deprivation is the main therapy currently in use for both primary and advanced PCA.¹ This treatment exerts its effect on target tissue by either blocking androgen [testosterone (T) and dihydrotestosterone (DHT)] synthesis or preventing binding of androgens to the androgen receptor (AR). The consequence of both strategies is interference with androgenic effects responsible for stimulation of prostate cancer cell growth. However, even the highly androgen-dependent cases of PCA that are initially responsive to androgen deprivation therapy eventually develop resistance due to selection or adaptation of androgen-independent clones.^{2,3} For these patients, no therapy

has been shown to be effective⁴ and new therapeutic strategies are urgently needed.

The androgen receptor (AR) is central to growth signaling in prostate cancer cells and experimental data suggest that the AR remains functional and active in androgen-independent/refractory prostate cancer through a variety of mechanisms aimed at increasing the growth response to lower levels of a wide variety of compounds.^{5–7} In the castrate environment, prostate cancer cells develop a growth advantage by amplifying or mutating the AR, altering AR co-regulatory molecules, and developing ligand-independent AR activation pathways.⁸ Indeed, the AR is expressed in all histological types and stages of PCA, including hormone refractory tumors.⁹ With this knowledge, it is reasonable to suggest that effective strategies (investigational new drugs) that lead to AR down-regulation and/or AR modulation may be useful for preventing the development, progression and proliferation of PCA.

From our research in the development of androgen synthesis inhibitors (CYP17 inhibitors) and anti-androgens

Keywords: Pharmacophore; Catalyst hypothesis; Androgen receptor down-regulating agents; Anti-prostate cancer agents.

* Corresponding author. Tel.: +1 410 706 5885; fax: +1 410 706 0032; e-mail: vnjar001@umaryland.edu

[†] These authors contributed equally to this work.

which are potential therapeutics for PCA,¹⁰ we became interested in the identification and development of novel agents capable of decreasing the expression and/or function of the AR. These compounds are hereafter referred to as androgen receptor down-regulating agents (ARDAs). Until recently, most of the known ARDAs were dietary compounds (natural products) including (–)-epicatechin (**1**), quercetin (**2**), curcumin (**3**), and vitamin E succinate (**4**).^{11–15} The potential implication of these dietary chemicals (nutraceuticals) on prevention of development and progression of PCA has recently been reviewed by Young et al.¹⁶ Other agents, such as flufenamic acid¹⁷ (**5**, a nonsteroidal anti-inflammatory agent) and LAQ824¹⁵ (a histone deacetylase inhibitor), have also been shown to decrease AR expression in LNCaP prostate cancer cells. The structures of these compounds are presented in Figure 1. All five compounds are found to decrease AR protein and mRNA expression. Furthermore, they were shown to decrease AR promoter activities as well. However, studies with these molecules have shown that the mechanism by which they potentiate their effects on the AR is not clear.^{11–14,17} Recent studies by Nelson and colleagues¹⁹ indicate that the anti-prostate cancer activities of *Scutellaria baicalensis*, a botanical with a long history of medicinal use in China, were attributed to four compounds that function in part through the inhibition of the AR signaling pathway. Interestingly, the four active compounds from this plant share the same flavone scaffold as that of epicatechin and quercetin. In addition, curcumin continues to be used as a lead compound to design and synthesize analogs as potential antiandrogenic agents for the treatment of prostate cancer.^{20–23}

A rational strategy for the identification of novel biologically active agents or leads with diverse chemical scaffolds is utility of three-dimensional (3D) generation and database searching. The increasing number of successful applications of 3D-pharmacophore-based

searching in medicinal chemistry clearly demonstrates its utility in the modern drug discovery paradigm.^{24–26} A pharmacophore is a representation of generalized molecular features including 3D (hydrophobic groups, charged/ionizable groups, hydrogen bond donor/acceptors), 2D (substructures), and 1D (physical and biological properties) aspects that are considered to be responsible for a desired activity. Two different approaches are applied in automated hypothesis generation. The first is Hypogen, an activity-based alignment derived from a collection of conformational models of compounds spanning activities of 4–5 orders of magnitude (the minimum number of molecules to ensure statistical significance of pharmacophores computed in the Catalyst Hypogen algorithm is 16). The second algorithm in 3D pharmacophore generation within Catalyst is a common feature based alignment of highly potent compounds. The activity of the molecules is not taken into consideration using this model generation mode. HipHop hypotheses are produced by comparing a set of conformational models and a number of 3D configurations of chemical features shared among the training set molecules. Compounds of the training set may or may not fit all features of resulting hypothesis, depending on the settings for the parameters Maximum Omitted Features, Misses, and Complete Misses. The retrieved pharmacophore models are expected to discriminate between active and inactive compounds.²⁷ Previously, we have successfully employed this strategy (HipHop) in the discovery of novel CYP17 inhibitors, potential therapeutics for PCA.²⁸ Considering the prospects of ARDAs as potential agents for the prevention and treatment of PCA as well as the paucity of potent ARDAs, we embarked on the use of Catalyst HipHop technology to generate a suitable pharmacophore model that may be useful for identifying novel ARDAs. In this paper, the generation of a pharmacophore model for ARDAs from a training set of five molecules using Catalyst/HipHop, the database search using an obtained

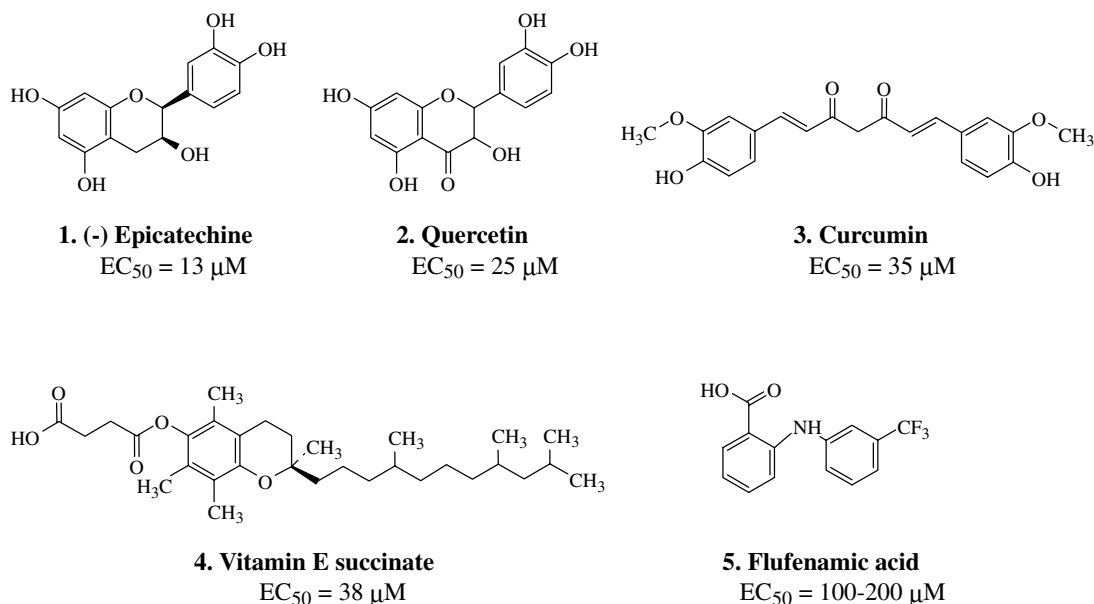


Figure 1. Chemical structures of five known androgen receptor down-regulating agents (ARDAs) used to generate the pharmacophore model.

pharmacophore model and the pharmacological results of the identified compounds, is discussed. A preliminary account of part of this work has been presented.²⁹

2. Results and discussion

2.1. Effects of ARDAs (training set compounds) on AR protein expression

Although the effects of known ARDAs on AR protein levels have been reported by various investigators,^{11–18} there are no reports of their EC_{50} values. All five known ARDAs (Fig. 1) were evaluated for their ability to decrease AR protein expression in a dose dependent manner and dose–response curves were generated to determine their EC_{50} values. Quercetin (2), the most well known naturally occurring AR down-regulating agent in LNCaP cells, was found to have an EC_{50} of about 25 μ M (Fig. 2). Quercetin, which is a naturally occurring flavanoid, has also been found to decrease the expression of the AR gene at the transcriptional level, thus it was of importance to include this molecule in the training set.¹² The EC_{50} values of all five compounds (13–200 μ M range) are presented in Table 1 and show that four out of five compounds, epicatechin (1), quercetin

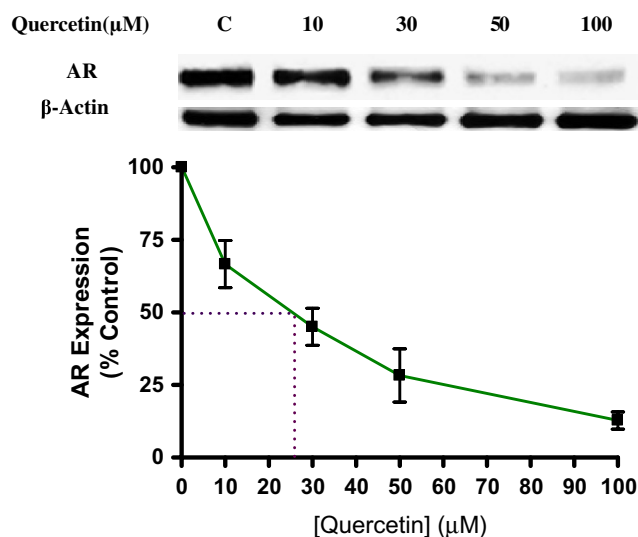


Figure 2. Dose-dependent androgen receptor down-regulation activity of quercetin (2) (determined by Western blot analysis). The experiments with the other agents (1, 3–5) gave plots that were essentially the same as shown above.

Table 1. EC_{50} values represent the ability of the compounds to decrease AR protein expression as determined by Western blotting

Compound	EC_{50} values (μ M)
Epicatechin (1)	13.0
Quercetin (2)	25.0
Curcumin (3)	35.0
Vitamin E succinate (4)	38.0
Flufenamic acid (5)	~200

These five known ARDAs were used to generate the training set of molecules.

(2), curcumin (3), and vitamin E succinate (4), exhibited low micromolar EC_{50} values. To the best of our knowledge, this appears to be the first report on EC_{50} values for AR protein expression of these well known ARDAs. Although we utilized the LNCaP cell line which contains a mutant AR, it should be noted that most ARDAs have been shown to exhibit similar effects on both the mutant and wild-type ARs.^{9,15} It should be stated that these compounds inhibit AR expression at both the transcription and translation levels or at either of these levels. The compounds in the training set possess diverse structures to furnish structural requirements for the three-dimensional pharmacophore model generation described hereafter.

2.2. Common feature-based pharmacophore model

The range of inhibitory activity (~ 2 log units) and a small set of molecules were not sufficient to allow us to generate a meaningful activity-based (predictive) pharmacophore model using Catalyst/Hypogen technology. However, on the basis of previous evidence of successful pharmacophore generation for molecules that do not act by the same mechanism of action, but differentially affect a particular molecular target,^{30,31} we employed the Catalyst/HipHop approach to evaluate the common feature required for binding and the hypothetical geometries adopted by these ligands in their most active forms. Thus, a training set consisting of five ARDAs (1–5, Fig. 1) with AR down-regulation activity through unknown mechanism was submitted for pharmacophore model generation based on common chemical features.

In the model generation methodology, the highest weight was assigned to the most active compound (–)epicatechin (1; EC_{50} = 13 μ M) in the training set. This was achieved by assigning a value of 2 (which ensures that all of the chemical features in the compound will be considered in building hypothesis space) and 0 (which forces mapping of all features of the compound) in the principle and maximum omitting features columns, respectively, for the most active compound. A value of 1 for the principle column ensures that at least one mapping for each of generated hypotheses will be found, and a value of 1 for the maximum omitting features column ensures that all but one feature must map for all other compounds (2–5) (for a detailed description of these input parameters, see the Catalyst 4.10 Tutorial). All other parameters were kept at the default settings. The 10 hypotheses (Hypo) generated had scores from 36.08 to 37.81 (Table 2). In this study, the Hypo1 is statistically best, and it maps to all the important features of the active compound and to some extent shows correlation between best fit values, conformational energies, and actual activities of the training set in comparison to other hypos (data not shown). This highest ranked pharmacophore hypothesis (Hypo1) was selected for the database search.

The selected pharmacophore model contained four chemical features: one hydrophobe (HYD), two hydrogen bond acceptors (HBA1 and HBA2), and one ring

Table 2. Summary of hypothesis run

Hypo	Feature ^a	Rank	Direct hit mask	Partial hit mask
1	RZHH	37.81	11111	00000
2	ZHHH	37.28	11011	00100
3	ZHHH	37.28	11011	00100
4	ZHHH	37.28	11011	00100
5	RZHH	36.95	11111	00000
6	ZHHH	36.45	11011	00100
7	ZHHH	36.45	11011	00100
8	ZDHH	36.19	01111	10000
9	ZDHH	36.19	01111	10000
10	ZHHH	36.08	11011	00100

In direct hit mask, (1) indicates every feature of training set molecule is mapped; (0) indicates 1 or more features were not mapped.

In partial hit mask, (0) indicates every feature of training set molecule is mapped; (1) indicates 1 or more features were not mapped.

^a Z; Hydrophobic (HYD), H; Hydrogen bond acceptor (HBA), D; Hydrogen bond donor, R; Ring aromatic (RA).

aromatic (RA) (Fig. 3). The HBA-1 maps the *meta*-hydroxy group of the aromatic ring attached to position 2 of the benzopyran ring of epicatechin, HBA-2 maps the hydroxyl group at position 3 of the benzopyran ring, the hydrophobic feature maps the aromatic ring attached to position 2 of the benzopyran ring, and ring aromatic maps the aromatic ring of benzopyran. The distance between RA and HBA1 or HBD was found to be 6.29 ± 1 Å and 5.67 ± 1 Å, respectively. The distance between HBA1 and HBA2 or HBD was found to be 5.02 ± 1 Å and 3.00 ± 1 Å, respectively. The distance between HBA2 and HBD or RA was found to be 4.46 ± 1 Å and 5.08 ± 1 Å, respectively. Figure 4 shows the alignment of (–) epicatechin (**1**) against Hypo1. This alignment represents a good match of features present in the ligand to the pharmacophore model (Fit score = 3.99/4). The mapping of Hypo1 onto (–) epicatechin was performed using the ‘Best Fit’ method in catalyst. During the fitting process, conformations on (–) epicatechin were calculated within the 20 kcal/mol energy threshold to minimize the distance between hypo features and mapped atoms of (–) epicatechin. Hypo1 has four features, and hence, the maximum fit value of any ligand alignment with this model would be 4.0. Alignment of Hypo1 with all training set

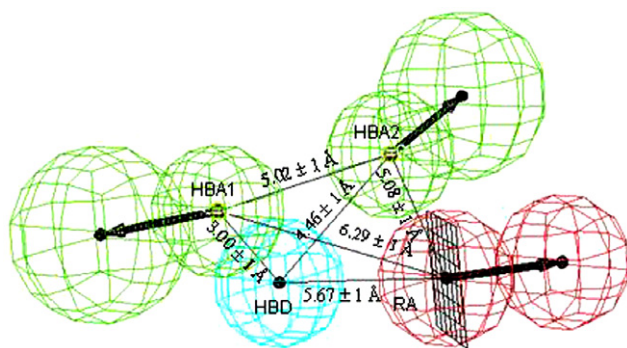


Figure 3. Common feature-based (Catalyst/HipHop) pharmacophore model of ARDAs. The model contains four features: one hydrophobic (cyan), two hydrogen bond acceptor (green), and one ring aromatic (red).

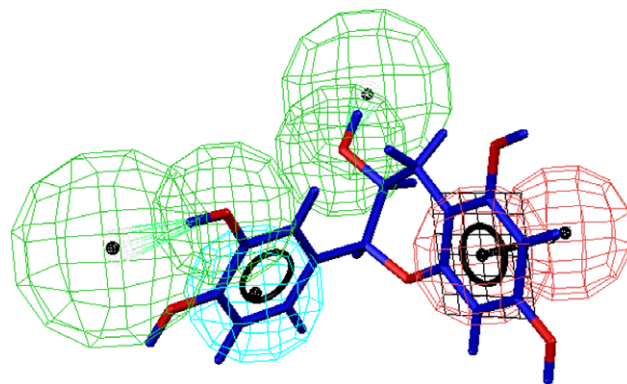


Figure 4. The mapping of the most active molecule of training set (–) epicatechin, **1**, to hypo1.

compounds was performed and found to give fit scores ranging from 3.05 to 3.99 (Fig. 5). The lowest fit score (3.05) corresponds to Flufenamic acid and explains the reason for its low activity.

To identify new ARDAs, Hypo1 was used as a search query against two databases: Catalyst/Maybridge 2003 (59,652 compounds) and NCI database (238,819 compounds). First, these two databases were filtered to seek out molecules having molecular weight (280–530), number of rotatable-bonds (5–27) and hetero-atoms (4–8) almost equal to the range of training set molecules. The search results are provided in Table 3. The hits retained for further evaluation were those with calculated fit score (of model alignment and ligand) greater than or equal to 3.05 [this is based on the lowest fit score from the alignment of the HipHop model with all five training set compounds (fit score range from 3.05 to 3.99)]. Seventeen compounds, presented in Figure 6a, were selected from the identified 41 compounds based on availability. The structures of these 17 compounds were different from those of the training set and other ARDAs. Compound NCI 0002205 possessed the highest fit value of 3.96 with the Catalyst generated pharmacophore model. The other retrieved molecules also displayed excellent fit values (3.37–3.96).

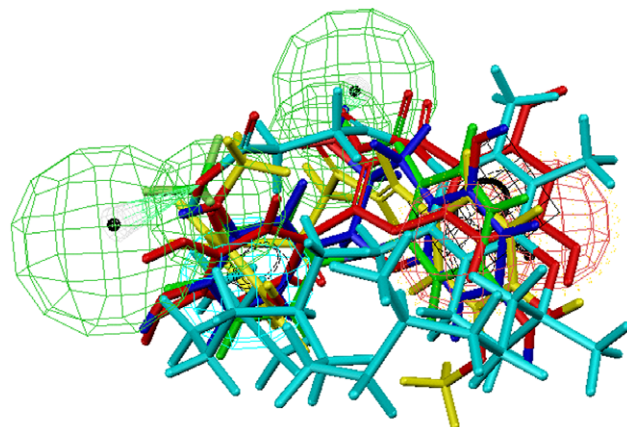


Figure 5. Alignment of common-feature pharmacophore model with training set ARDAs.

Table 3. Results of 3-D search of two databases (NCI and Maybridge) using the pharmacophore model derived for ARDAs (Hypo 1) as search query

Database	DB size	Filtered	No. of hits	% of databases	Hits with fit score >3.05
NCI	238,819	44,236	93	0.038	29
Maybridge2003	59,652	5000	48	0.08	12

2.3. Biological studies with compounds identified using Catalyst

An initial screening of these 17 compounds at concentrations of 50 and 150 μM for their abilities to cause down-regulation of AR protein expression resulted in the identification of only six active compounds. The 2D mapping of these six compounds is shown in Figure 6b. These compounds were further evaluated to determine their EC_{50} values (from dose–response curves). The EC_{50} values (17.5–212 μM range) as presented in Table 4 show that the compounds exhibited EC_{50} values in a range similar to the range of values of the training set compounds used to generate the ARDA pharmacophore model. KM06622 (Maybridge) was the most potent with an EC_{50} value of 17.5 μM . Dose-dependent

androgen receptor down-regulation activity of NCI 0002815 (determined by Western blot analysis) is shown in Figure 7. The experiments with the other five agents gave similar plots. We note that there is no obvious structure activity relationship (SAR) with this set of newly identified ARDAs.

These compounds were also evaluated for their abilities to inhibit the viability of LNCaP cells. Except for KM06622, the other five compounds exhibited strong inhibition (IC_{50} values 4.5–39.8 μM) of LNCaP cell growth (Table 4). Dose-dependent curve for inhibition of human prostate LNCaP cells by NCI 0002815 is shown in Figure 8. The experiments with the other five agents gave plots that were similar. These findings are significant because of previous reports that the

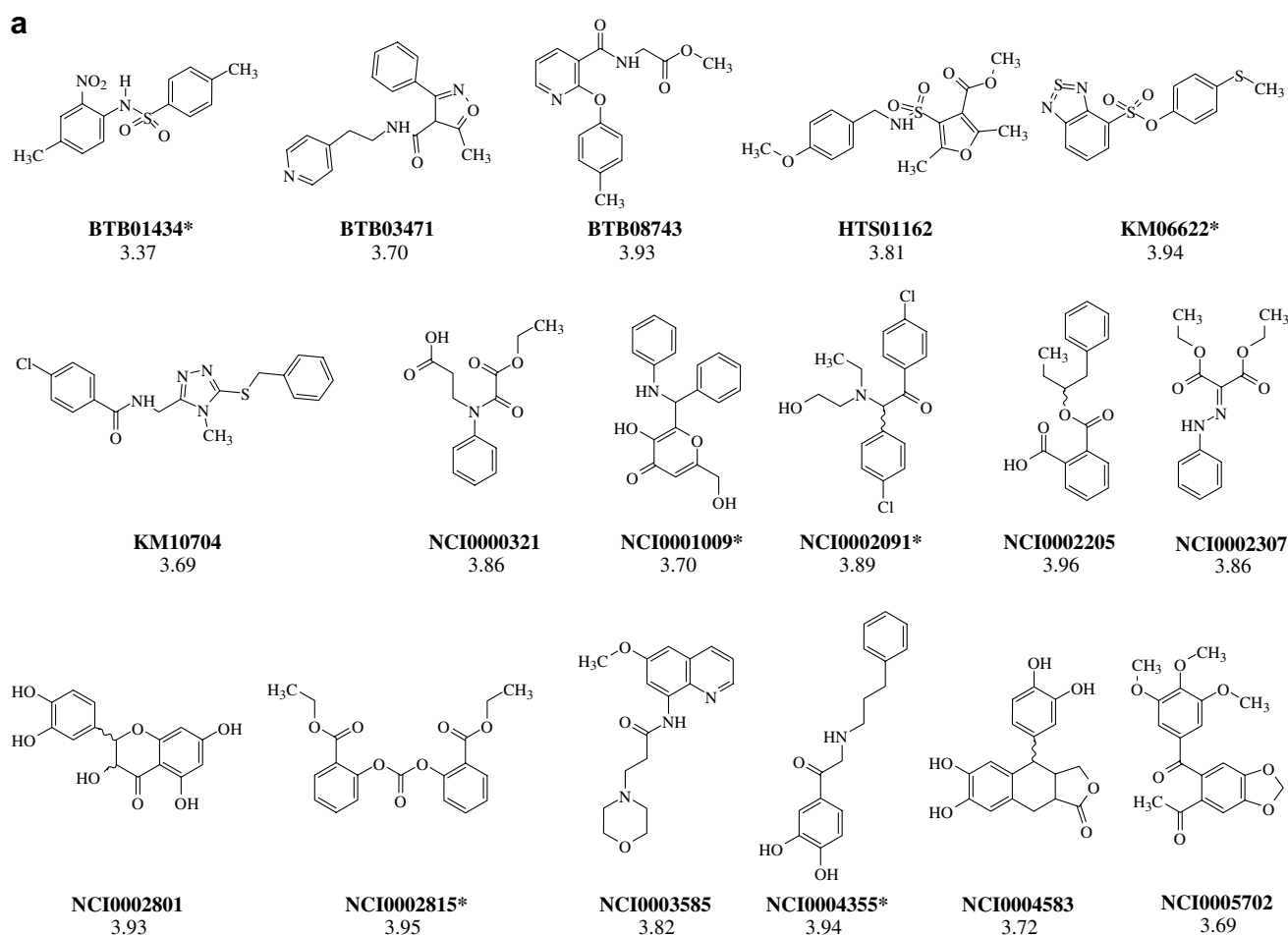


Figure 6. (a) Structures of some compounds (17) retrieved as 'hits' from 3D search of Catalyst formatted NCI and Maybridge Databases using the generated pharmacophore model. The star sign (*) indicates compounds (six) that were found to possess significant androgen down-regulating activities. (b) 2D mapping of training set and retrieved molecules showing androgen receptor down-regulation activity with chemical features of Hypo1.

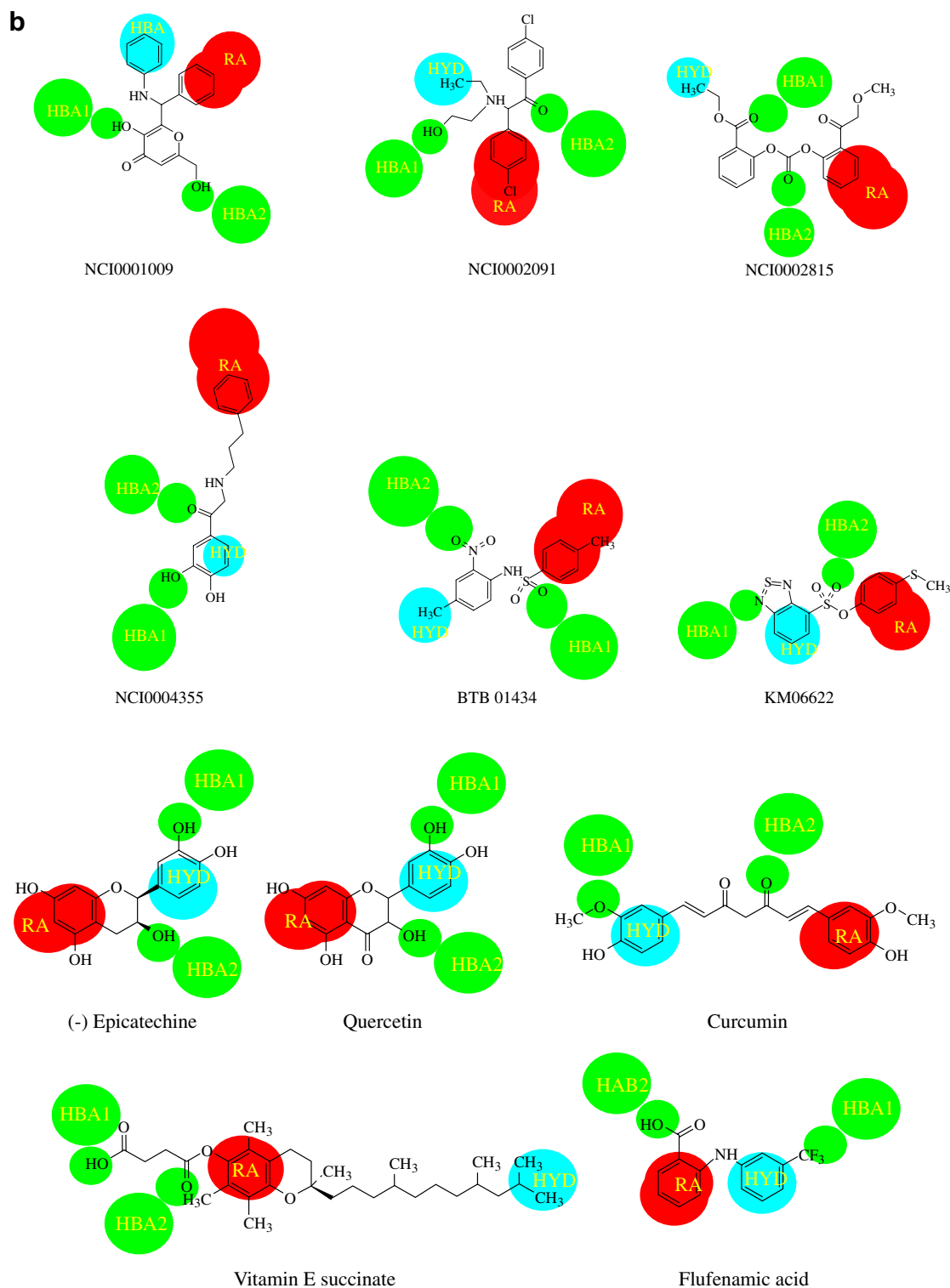


Figure 6. (continued)

well-known natural products ARDAs, such as quercetin, curcumin, and others, inhibit the growth of human cancer cells at relatively high μM concentrations.^{12,14,16} Interestingly, ARDA activity did not correspond to inhibition of cell viability in LNCaP cells, however, future studies with these new ARDAs would investigate the mechanism by which they inhibit the growth of human prostate cancer cells and tumors.

3. Conclusions

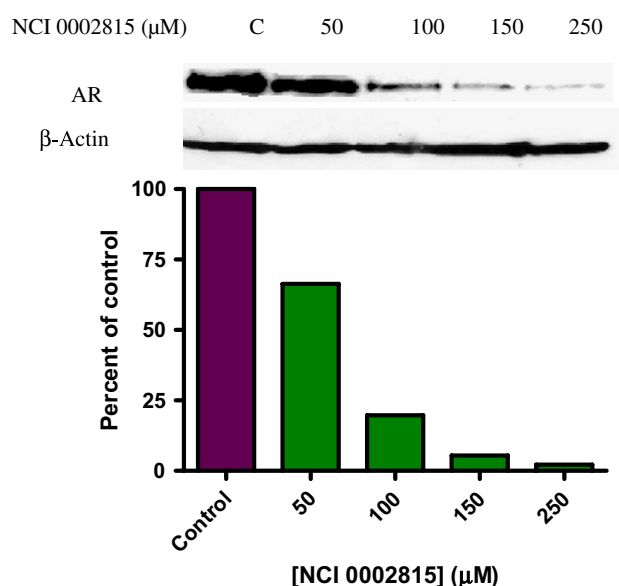
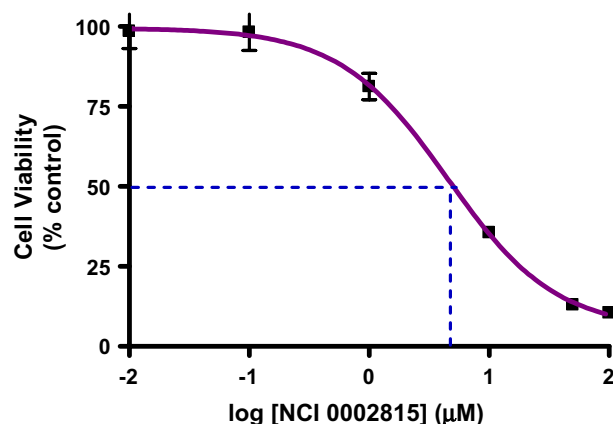
The present study is the first successful example for a rationale identification of androgen receptor down-regulating agents (ARDAs). This was accomplished by generating a three-dimensional pharmacophore model based on a training set of five well-known ARDAs. The model containing one hydrophobic group, one aro-

Table 4. Six ARDAs identified by the generated pharmacophore model

Compounds	EC ₅₀ ^a (μM)	IC ₅₀ ^b (μM)
NCI-0001009	212	20.9
NCI-0002091	39.5	8.31
NCI-0002815	65.5	4.5
NCI-0004355	43.5	26.9
BTB 01434	76	39.8
KM 06622	17.5	>50

^a EC₅₀ values represent the ability of the compounds to down-regulate AR protein expression.

^b IC₅₀ values are indicative of the effect of the molecules on LNCaP cell viability. All values are indicated as percent of control.

**Figure 7.** Dose-dependent androgen receptor down-regulation activity of NCI 0002815 (determined by Western blot analysis). The experiments with the other five agents gave similar plots.**Figure 8.** Dose-dependent curve for inhibition of human prostate LNCaP cells by NCI 0002815. The experiments with the other five agents gave plots that were similar.

matic group, and two hydrogen bond acceptors identified 93 and 48 compounds from the NCI (59,652 compounds) and Maybridge (238,819 compounds) databases, respectively. The study resulted in the

identification of six small molecules that were experimentally confirmed as ARDAs and the compounds also exhibited significant human prostate cancer LNCaP proliferation inhibitory activities. These new scaffolds can be used as leads for rational design of potent ARDAs and hence anti-prostate cancer agents.

4. Experimental

4.1. Cell culture

Androgen-dependent LNCaP cells were obtained from American Type Culture Collection (Rockville, MD, USA). Cells were maintained in RPMI 1640 medium supplemented with 10% fetal bovine serum (Atlanta Biologicals, Lawrenceville, GA, USA) and 1% penicillin/streptomycin. Cells were grown as a monolayer in T75 or T150 tissue culture flasks in a humidified incubator (5% CO₂, 95% air) at 37 °C.

All ARDA compounds were obtained from either the NCI (National Institutes of Health, Bethesda, MD, USA) or Maybridge (Ryan Scientific, Inc., Isle of Palms, SC, USA) databases.

4.2. Western blot analysis

For immunoblot detection of the AR, LNCaP cells were cultured as described above in T25 flasks. Cells were treated with various concentrations of ARDAs and whole cell lysates were prepared using lysis buffer containing 0.1 M Tris, 0.5% Triton X-100, and protease inhibitor. Protein content was determined using the Bradford Assay (Bio-Rad, Hercules, CA, USA). Protein was subjected to SDS-PAGE (10% acrylamide) and transferred onto nitrocellulose membrane. The blots were blocked overnight in 5% nonfat milk in PBS-T buffer at 4 °C. Monoclonal antibody was used against the AR (AR441; sc-7305; Santa Cruz Biotechnology, Santa Cruz, CA; 1:500 dilution) at room temperature for 1 h. Membranes were then incubated with a goat anti-mouse IgG secondary antibody conjugated to horseradish peroxidase (Bio-Rad Cat. #170-6516; 1:2000 dilution) at room temperature for 1 h. Blots were rinsed with PBS-T between each step and specific bands were visualized by enhanced chemiluminescence (ECL; Amersham Biosciences, Arlington Heights, IL, USA). Equivalent loading of samples was determined by reprobing membranes with β-actin (Calbiochem, USA). Protein expression was normalized to β-actin.

4.3. Cell growth inhibition (MTT colorimetric assay)

LNCaP cells were seeded in 24-well plates (Corning Costar) at a density of 2×10^4 cells per well per 1 mL of medium. Cells were allowed to adhere to the plate for 24 h and then treated with different concentrations of ARDAs dissolved in DMSO. Cells were treated for five days with renewal of ARDA and media on day 3. On the fifth day, medium was renewed and 100 μL of MTT (3-(4,5-dimethylthiazol-2-yl)-2,5-diphenyl-2H-tetrazolium bromide from Sigma) solution (0.5 mg

MTT/mL of medium) was added to the medium such that the ratio of MTT:medium was 1:10. The cells were incubated with MTT for 2 h. The medium was then aspirated and 500 μ L DMSO was added to solubilize the violet MTT-formazan product. The absorbance at 560 nm was measured by spectrophotometry (Victor 1420 multilabel counted, Wallac). For each concentration of ARDA there were triplicate wells in each independent experiment. IC₅₀ values were calculated by nonlinear regression analysis using GraphPad Prism software.

4.4. Computational methods

All molecular modeling studies were performed using Catalyst 4.10³² installed on Silicon Graphics O₂ workstation equipped with a 300 MHz MIPS R5000 processor (128 MB RAM) running the Irix 6.5 operating system.

All structures were generated using 2D/3D editor sketcher and minimized to the closest minimum using the CHARMM-like force field implemented in the program.³³ Regarding the asymmetric centers of all the compounds, as we tested *ss* isomer of (–)-epicatachin we assigned *ss* for epicatachin, whereas for quercetin and vitamin E succinate, it was arbitrarily decided to assign ‘undefined’ chirality, allowing the pharmacophore model to choose which configuration of the asymmetric carbon atoms is the most appropriate. A stochastic research coupled to a poling method³⁴ was applied to generate conformers for each compound by using ‘Best conformer generation’ option with a 20 kcal/mol energy cutoff (20 kcal/mol maximum compared to the most stable conformer).

The pharmacophore-based investigation of ARDAs involved using the Catalyst/HipHop program to generate feature-based 3D pharmacophore alignments.^{35,36} This was performed in a three-step procedure³⁷: (a) a conformation model for each molecule in the training set was generated; (b) each conformer was examined for the presence of certain chemical features; (c) a three-dimensional configuration of chemical features common to the input molecules was determined. Catalyst provides a dictionary of chemical features found to be important in drug-enzyme/receptor interactions. These are hydrogen bond donors (HBD), hydrogen bond acceptors (HBA), hydrophobic group (HYD), ring aromatic (RA), and positive (PI) and negative ionizable (NI) groups. For the pharmacophore modeling runs, common features selected for the run were ring aromatic (R), hydrogen bond donor (D), hydrogen bond acceptor (H), hydrophobic group (Z), and negative ionizable group (N). The default HBA of the feature dictionary which recognizes N, O, and S as hydrogen bond acceptors was modified to include ‘F’, as Flufenamic acid (molecule 3 of Table 1) contains trifluoromethyl group based on electronegativity differences, ‘F’ is also thought to act as hydrogen bond acceptor.

There are two strategies for HipHop model generation. The first one assumes that ‘all compounds are

important and contain important features, furthermore, differences in activities are related to the differences in other relevant factors like conformational energies, but not due to the absence of any important features required for binding’. In contrast, the hypothesis generation in the second strategy gives bias to the most active compounds assuming that they contain all important features and remaining compounds may or may not contain important features.³⁸ Since there is considerable difference in AR down-regulation activity between the most and least active molecules of the training set, we assume that adapting strategy II (giving bias to most active molecule) will provide pharmacophore with additional feature if any, which may not be present in least active compounds.

Acknowledgments

This research was supported in part by a grant from US National Institutes of Health and National Cancer Institute (R21 CA117991-01) to VCON. RDB is supported by a training grant by the National Institute of Environmental Health Sciences (2T32ES007263-16A1). We thank the agency for their generous support.

References and notes

1. Cancer Statistics 2005; American Cancer Society: Washington, DC, 2006.
2. Isaacs, J. T.; Coffey, D. S. *Cancer Res.* **1981**, *41*, 4070–5075.
3. Bruchovsky, N.; Rennie, P. S.; Coldman, A. J.; Goldenberg, S. L.; To, M.; Lawson, D. *Cancer Res.* **1990**, *50*, 2275–2282.
4. Ferrari, A. C.; Chachoua, A.; Singh, H.; Rosenthal, M.; Taneja, S.; Bendnar, M.; Mandeli, J.; Muggia, F. *Cancer* **2001**, *91*, 2039–2045.
5. Taplin, M.-E.; Balk, S. P. *J. Cell. Biochem.* **2004**, *91*, 483–490.
6. Santos, A. F.; Huang, H.; Tindall, D. J. *Steroids* **2004**, *69*, 79–85.
7. Chen, C. D.; Welsbie, D. S.; Tran, C.; Baek, S. H.; Chen, R.; Vessella, R.; Rosenfeld, G. M.; Sawyer, C. L. *Nat. Med.* **2004**, *10*, 33–39.
8. Suzuki, H.; Ueda, T.; Ichikawa, T.; Ito, H. *Endocr. Rept. Cancer* **2003**, *10*, 209–216.
9. Mohler, J. L.; Gregory, C. W.; Harris, O., III; Kim, D.; Weaver, C. M.; Petrusz, P.; Wilson, E. M.; French, F. S. *Clin. Cancer Res.* **2004**, *10*, 440–448.
10. Handratta, V. D.; Vasaitia, T. S.; Njar, V. C. O.; Gediya, L. K.; Kataria, R.; Chopra, P.; Newman, D., Jr.; Farquhar, R.; Guo, Z.; Qiu, Y.; Brodie, A. M. H. *J. Med. Chem.* **2005**, *48*, 2972–2984.
11. Ren, F.; Zhang, S.; Mitchell, S. H.; Butler, R.; Young, C. Y. F. *Oncogene* **2000**, *19*, 1924–1932.
12. Xing, N.; Chen, Y.; Mitchell, S. H.; Young, C. Y. F. *Carcinogenesis* **2001**, *22*, 409–414.
13. Zhang, Y.; Ni, J.; Messing, E. M.; Chang, E.; Yang, C.-R.; Yeh, S. *Proc. Natl. Acad. Sci. U.S.A.* **2002**, *99*, 7408–7413.
14. Nakamura, K.; Yasunaga, Y.; Segawa, T.; Ko, D.; Moul, J. W.; Srivastava, S.; Rhim, J. S. *Int. J. Oncol.* **2002**, *21*, 830–852.

15. Thompson, T. A.; Wilding, G. *Mol. Cancer Ther.* **2003**, *2*, 797–803.
16. Young, C. Y.; Jatoi, A.; Ward, J. F.; Blute, M. L. *Curr. Med. Chem.* **2004**, *7*, 909–923.
17. Zhu, W.; Smith, A.; Young, C. Y. F. *Endocrinology* **1999**, *140*, 5451–5454.
18. Chen, L.; Meng, S.; Wang, H.; Bali, P.; Bai, W.; Li, B.; Atadja, P.; Bhalla, K. N.; Wu, J. *Mol. Cancer Ther.* **2005**, *4*, 1311–1319.
19. Bonham, M.; Posakony, J.; Coleman, I.; Montgomery, B.; Simon, J.; Nelson, P. S. *Clin. Cancer Res.* **2005**, *11*, 3905–3914.
20. Ohtsu, H.; Itakawa, H.; Xiao, Z.; Su, C.-Y.; Shih, C. C. Y.; Chiang, T.; Chang, E.; Lee, Y.; Chiu, S.-Y.; Chang, C.; Lee, K.-H. *Bioorg. Med. Chem.* **2003**, *11*, 5083–5090.
21. Ohtsu, H.; Xiao, Z.; Ishida, J.; Naggai, M.; Wang, H.-K.; Itakawa, H.; Su, C.-Y.; Shih, C.; Chiang, T.; Chang, E.; Lee, Y.; Tsai, M.-Y.; Chang, C.; Lee, K.-H. *J. Med. Chem.* **2002**, *45*, 5037–5042.
22. Lin, L.; Shi, Q.; Su, C.-Y.; Shih, C. C. Y.; Lee, K.-H. *Bioorg. Med. Chem.* **2006**, *14*, 2527–2534.
23. Lin, L.; Shi, Q.; Nyarko, A. K.; Bastow, K. F.; Wu, C.-C.; Su, C.-Y.; Shih, C. C.-Y.; Lee, K.-H. *J. Med. Chem.* **2006**, *49*, 3963–3972.
24. Guner, O. F. *Pharmacophore Perception, Development, and Use in Drug Design*; International University Line: La Jolla, CA, 2000.
25. Dror, O.; Shulman-Peleg, A.; Nussinov, R.; Wolfson, H. L. *Curr. Med. Chem.* **2004**, *11*, 71–90.
26. Lyne, P. D.; Kenny, P. W.; Cosgrove, D. A.; Deng, C.; Zabudoff, S.; Wendoloski, J. J.; Ashwell, S. *J. Med. Chem.* **2004**, *47*, 1962–1968.
27. Kovat, E. M.; Langer, T. *J. Med. Chem.* **2003**, *46*, 716–726.
28. Clement, O. O.; Freeman, C. M.; Hartmann, R. W.; Handratta, V. D.; Vasaitis, T. S.; Brodie, A. M. H.; Njar, V. C. O. *J. Med. Chem.* **2003**, *46*, 2345–2351.
29. Njar, V. C. O.; Purushottamachar, P.; Khandelwal, A.; Maheshwari, N.; Chopra, P.; Gediya, L. K. *232nd American Chemical Society (ACS) National Meeting*, San Francisco, CA, USA, September 10–14, 2006, Abstract #MEDI 75.
30. Bahattacharjee, A. K.; Dheranetra, W.; Nichols, D. A.; Gupta, R. K. *QSAR Comb. Sci.* **2005**, *24*, 593–602.
31. Delfin, D. A.; Bahattacharjee, A. K.; Yakovich, A. J.; Werbovetz, K. A. *J. Med. Chem.* **2006**, *49*, 4196–4207.
32. *Catalyst*, release version 4.10; Accelrys, 9685 Scranton Road, San Diego, CA 92121.
33. Brooks, B. R.; Bruccoleri, R. E.; Olafson, B. D.; States, D. J.; Swaminathan, S.; Karplus, M. *J. Comput. Chem.* **1983**, *4*, 187–217.
34. Smellie, A.; Teig, S. L.; Towbin, P. *J. Comput. Chem.* **1995**, *16*, 171–187.
35. Sprague, P. W. Automated Chemical Hypothesis Generation and Database Searching with Catalyst. In *Perspectives in Drug Discovery and Design*; Müller, K., Ed.; ESCOM Science Publishers B.V.: Leiden, The Netherlands, 1995; Vol. 3, pp 1–20.
36. Greene, J.; Kahn, S.; Savoj, H.; Sprague, P.; Teig, S. *J. Chem. Inf. Comput. Sci.* **1994**, *34*, 1297–1308.
37. Clement, O. O.; Trope-Mehl, A. HipHop: Pharmacophores Based on Multiple Common-feature Alignments. In *Pharmacophore Perception, Development, and Use in Drug Design*; Güner, O. F., Ed.; International University Line: La Jolla, CA, 2000; pp 69–83.
38. Doddareddy, M. R.; Jung, H. K.; Lee, J. Y.; Lee, Y. S.; Cho, Y. S.; Koh, H. Y.; Pae, A. N. *Bioorg. Med. Chem.* **2004**, *12*, 1605–1611.